Supporting Information

Rational design of light induced self healed Fe based oxygen vacancy rich CeO_2 (CeO_2NS-FeOOH/Fe_2O_3) nanostructure materials for photocatalytic water oxidation and Cr(VI) reduction.

S. Sultana, S. Mansingh, and K. M. Parida *

Centre for Nano Science and Nano Technology SOA Deemed to be University, Bhubaneswar—751 030, Odisha (India)

Materials & Experimental Procedure

Chemicals:

$Ce(NO_3)_3.6H_2O$, $Fe(NO_3)_3.9H_2O$, Na_2CO_3, NaOH, KOH and $AgNO_3$ were purchased from Merck India. All the chemicals were used in this work were of analytical grade (Merck) and were used as received without further purification. Doubly distilled water was used throughout the experiments.

Sample Preparation

α-FeOOH nanorods

α-FeOOH was prepared by simple hydrothermal technique based on our previous paper. 1.237g of $Fe(NO_3)_3.9H_2O$ was dissolved in 20mL of water under magnetic stirring. Then 0.5M NaOH solution was added slowly on to the dissolved Fe(III) solution till its pH was raised upto 12 under vigorous stirring. Then the suspension solution was transferred to a Teflon lined steel autoclave of 120mL capacity and maintained at 180^0C for 24h. After it cooled down to room temp the red product was separated by centrifugation and washed several times with water and further dried in oven for 24h at 60^0C.

CeO_2 Nanosheets

Ceria nanosheets were prepared by simple precipitation technique followed by calcinations. First 200mL aqueous solution containing 16mM $Ce(NO_3)_3$ and 52mM sodium carbonate were prepared individually. Then sodium carbonate solution was added drop wise in to the cerium nitrate solution under stirring. Gradually a white precipitate was formed and was stirred for 2h in an ice cold water bath. Then the as obtained precipitate was aged for another 15h at 4^0C. The final product was collected by centrifugation, washed several times with distilled water and then dried at 110^0C over night in a hot air oven. Finally, the dried sample was ground into the powder and was added to a crucible, calcined at 450^0C for 4h at a rate of 5^0C/min in muffle furnace.

α-FeOOH/CeO_2NS and αFe_2O_3/CeO_2NS

The binary hybrid was prepared by insitu production of ironoxyhydroxide from iron(III) solution in presence of CeO_2NSs. 0.25g of CeO_2NS was added into the beaker containing an aqueous suspension containing iron(III) precipitate of pH12 under magnetic stirring. Additional 30min sonication was done in order to homogenize the solid solution mixture. Then the homogeneous suspension was kept in autoclave for same 24h at 180^0C. After it cooled down to room temp the resulting precipitate was separated and washed several times with distilled water then dried at 60^0C. The sample was labelled as αFeOOH/CeO_2NSs. For αFe_2O_3/CeO_2NS, CeO_2NS were dispersed in the beaker containing 20mL of water. Then calculated amount of iron nitrate solids are taken in it. Then the pH of the solution was adjusted to 12 and was stirred additionally for 12h more. Then the solution was kept in autoclave for 28h at 180^0C and was further aged for 24h. Then the precipitates were collected and washed with distilled water and kept in oven for further use.

Materials Charecterization

The XRD characterization was carried out by Rigaku Miniflex XRD instrument with Cu (Kα) radiation (λ=0.15418 nm) from 10˚ to 80˚ at a scan rate of 2º/min. By using JASCO V-750 spectrophotometer the UV-visible diffuse reflectance spectrum was obtained in the range of 200 to 800 nm. The photoluminescence properties were evaluated by using a JASCO FP-8300 spectrofluorimeter with an excitation wavelength of 320nm. XPS characterization was done by using

Kartos axis ultra Xray photoelectron spectrometer system consisting of a charge neutralizer and Al Kα X-ray monochromatizating source. The transmission electron microscopy (TEM) images were carried on a Philips TECNAI G^2 electron microscope operated at an accelerating voltage of 200 kV. All photoelectrochemical studies were carried out on IVIUMn STAT and the working electrode was prepared through electrochemical deposition technique on the surface of FTO. The counter and reference electrode were Pt electrode and Ag/AgCl whereas 300 W Xe lamp was used as the light source. The Nyquist plot was done at 10^5 Hz to 10^2 Hz at zero bias in 1MKOH in the presence of light at open circuit potential. The linear sweep voltammetry (LSV) plots were evaluated by sweeping the potential from -0.5 to 1V in the solution containing 1MKOH electrolyte.

Photocatalytic Cr(VI) reduction reaction

The photocatalytic activity of the materials was evaluated by monitoring the reduction of Cr(VI) under the irradiation of direct solar light. Initially 10mg/L concentration of Cr(VI) stock solution was prepared and for each experiment 50mg of solid catalysts were dispersed in the 50 mL of prepared stock solution. Then the dispersed solutions were stirred in the dark for 30mins in order to achieve the sorption equilibrium. Then, 0.05 g citric acid was added to the suspension. After that the above solutions were kept in solar light with slow stirring. The photoreduction process was analyzed by monitoring the decrease concentration of Cr(VI) through JASCO 750 UV-visible spectrophotometer. The concentration of Cr(VI)-DPC solution was determined by monitoring the absorbance of at 540 nm. Blank test were also performed in the absence of photocatalysts. After each cycle, the catalyst was recollected by centrifugation and washing, then tested the next cycle.

Photocatalytic Water oxidation reaction

The photocatalytic O_2 evolution reaction was carried out in a 100 mL sealed quartz batch reactor round bottom flask with 150W Xe lamp as the irradiating source. The light source was kept 10cm away from the bottom of the reactor and adjusted 8.9cm above from the aqueous suspension. The reaction was examined by dispersing 20 mg as synthesized powdered catalyst into 20 mL aqueous solution containing 0.05M $AgNO_3$/$FeCl_3$ with constant stirring in order to maintain the uniformity of

suspension throughout the whole reaction. Before light irradiation, N_2 gas was purged for 30 mins through the reactor in order to completely remove all dissolved oxygen. The amount of oxygen gas was evolved which was determined thoroughly measured by collecting the gas via downward displacement of water and analysed by gas chromatography.

Photocatalytic Cr(VI) Reduction

Here we have adopted a green method i.e. photocatalytic reduction of Cr(VI) to Cr(III) over our as prepared catalysts. It was seen that the reduction of Cr(VI) hardly occurred in the absence of photocatalysts. However, under direct sunlight nanohybrids showed remarkable reduction efficiency as compared to its neat material without maintaining the pH. It was well known that the pH value of reaction medium also play a crucial role in the photo-reduction of Cr(VI). So at first the effect of the solution pH on the photocatalytic reduction of Cr(VI) was investigated for $FeOOH/CeO_2$ sample under visible light as shown in Fig. S4(a). It could be observed that at lower pH (pH = 2) photocatalytic reduction of Cr(VI) is highest i.e 99%, while the reduction rate was only 59% at pH = 10 within 40 min. Thus, the higher rate of Cr(VI) degradation is proved to be at lower pH, which is due to the accumulation of more positive charges over the photocatalyst surface leading to strong electrostatic binding of the negatively-charged $HCr_2O_7^-$ species. Therefore photoreduction Cr(VI) of all the samples were carried out in pH 2 for a time period of 40 min. It is more convincing that $FeOOH/CeO_2$ and Fe_2O_3/CeO_2 displayed the best photocatalytic performance with a reduction rate of 99.7% and 94.5% respectively as shown in fig. S4(b). While, the pristine CeO_2 exhibited a lower degradation efficiency because of its UV active nature and rapid excitons recombination, but some Cr(VI) were photoreduced on the surface of CeO_2 due to Ce^{3+} and surface defects under direct sunlight. Whereas visible light active FeOOH exhibited a moderate reduction ratio of Cr(VI) (approximately 69%) under the same conditions, due to the rapid recombination of photo-generated electron-hole pairs. Fig. S4(c) shows the time-dependent reduction curves of Cr(VI) within 40 min for $FeOOH/CeO_2$. It was clearly observed that with the increase in light irradiation time upon Fe-CeO_2NS, the peak intensity at 540nm of hexavalent Cr(VI) gradually decreases and also the colour of the chromium complex solution(DPC-Cr(VI)) change from pink to colourless which indicate the

successful reduction of Cr(VI) to Cr(III). The obtained results are encouraging because of the absence of any reducing agent such as $NaBH_4$ [1]. Further by plotting the lnC/C0 graph of the obtain results, it was confirmed that the reaction follow pseudo-first-order. The kinetic plots and rate constant 'k' of Cr(VI) reduction with different photocatalysts are shown in fig. S4(d)The rate constant 'k' of $FeOOH/CeO_2$ reached 0.143 min^{-1} which is approximately 20.4, 5.95 and 1.45 times higher than that of CeO_2, FeOOH and Fe_2O_3/CeO_2 respectively. In addition to photocatalytic activity, the photostability of photocatalyst is another important factor. In order to analyze the photostability of the catalyst, four cycles of photoreduction experiments one following the other have been carried out for $FeOOH\text{-}CeO_2$ (fig. S4 (e)). From the repeated experiments it was concluded that the photocatalyst still maintained a high level of reduction ability in the repeated experiments.

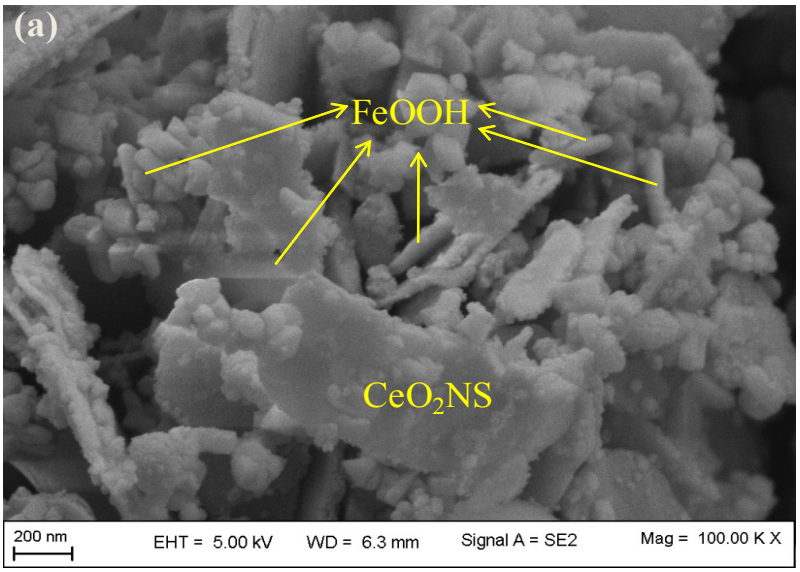

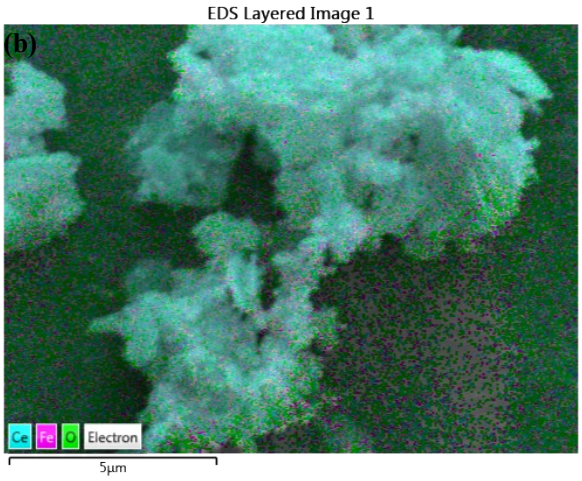

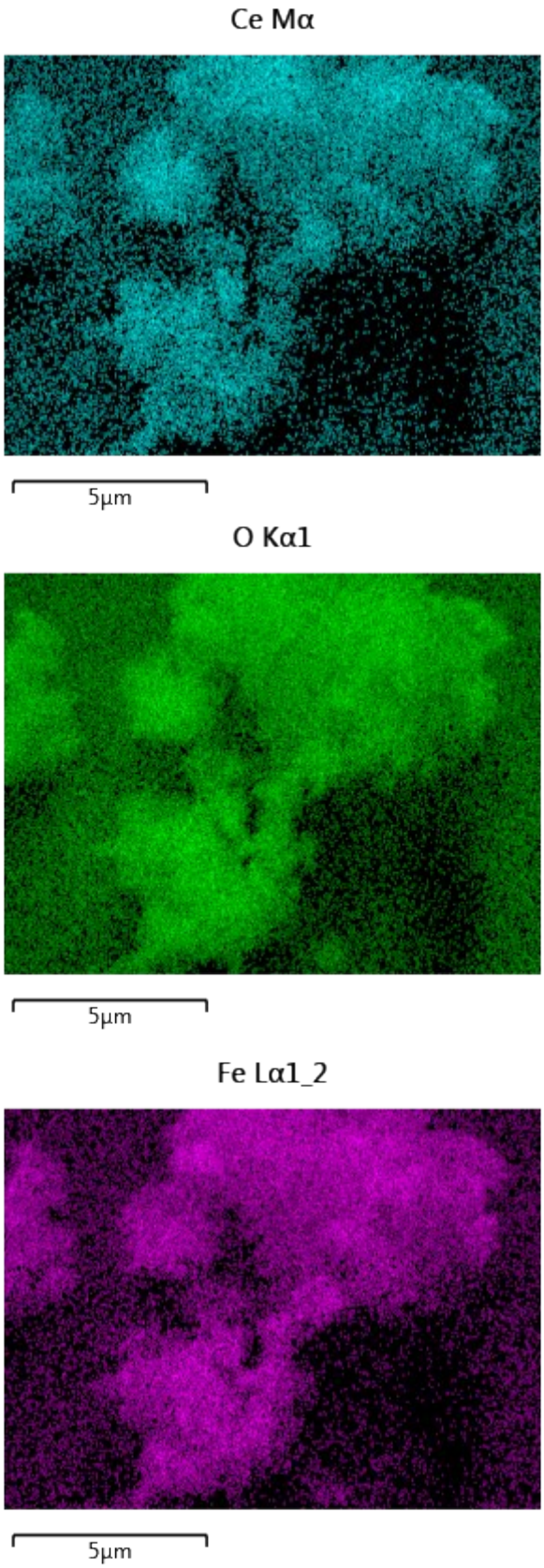

Fig. S1 (a) FESEM image of α-FeOOH/CeO_2NS heterostructure (b) Colour elemental mapping of α-FeOOH/CeO_2NS heterostructure showing Ce, Fe and O distribution.

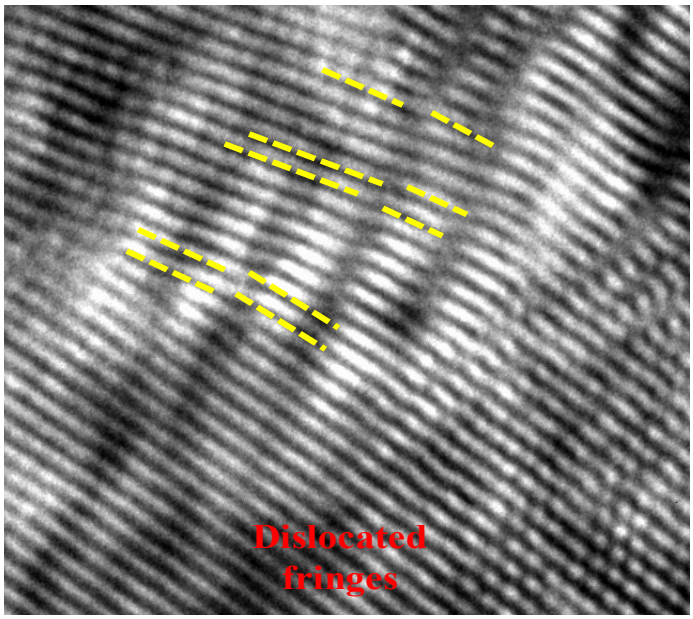

Fig. S2 HRTEM image of dislocated fringes of CeO_2 in α-Fe_2O_3/CeO_2NS.

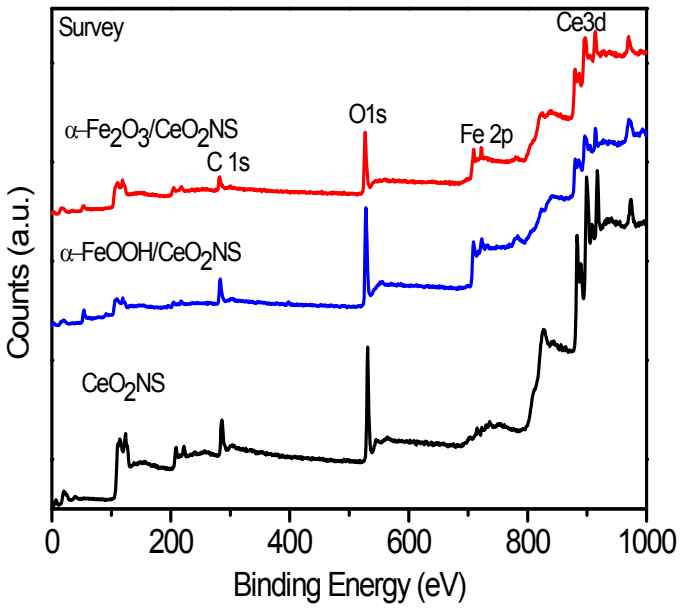

Fig. S3 XPS survey spectrum of CeO_2, α-FeOOH/CeO_2 NS and α-Fe_2O_3/CeO_2NS.

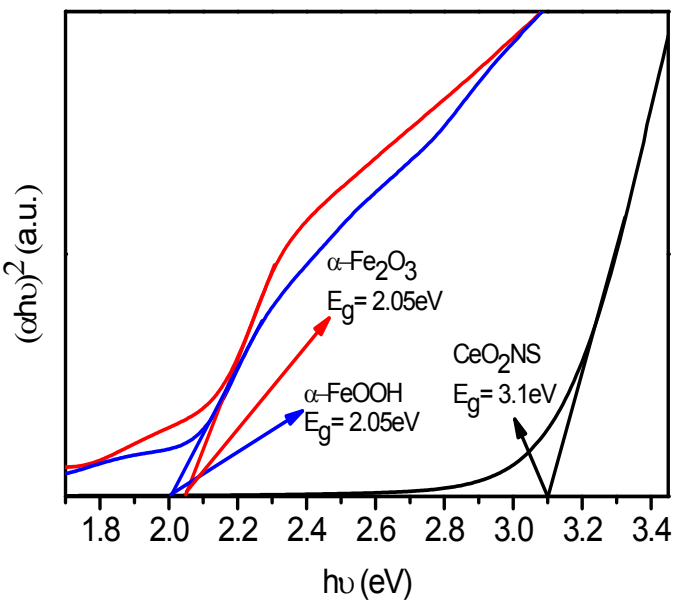

Fig. S4 Band gaps of neat CeO_2NS, α-FeOOH and α-Fe_2O_3.

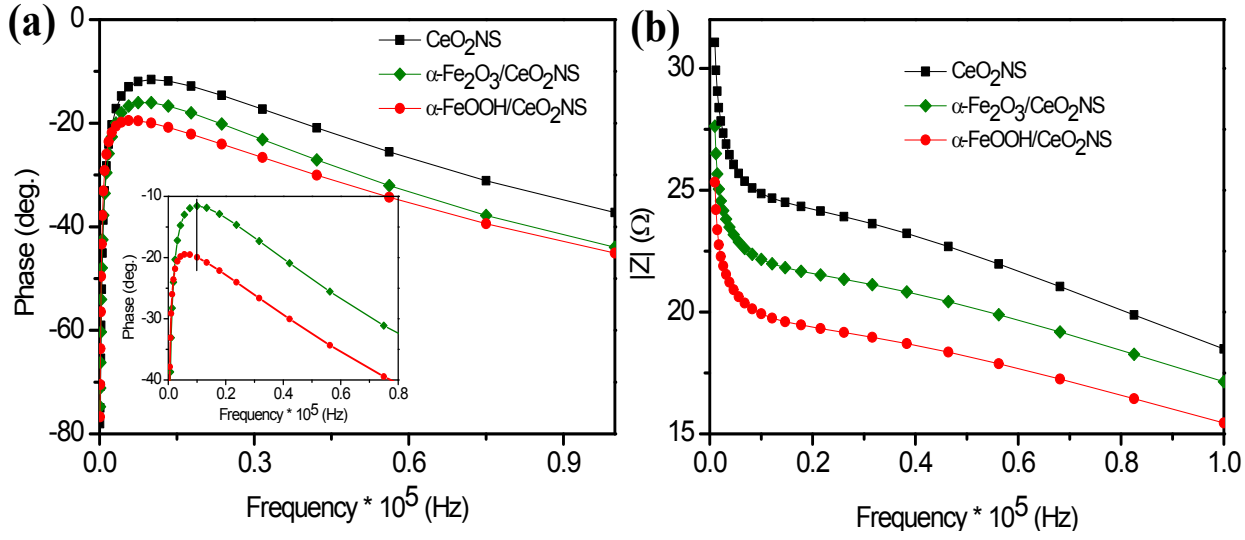

Fig. S5 (a) and (b) Bode's phase plot of CeO_2, α-FeOOH/CeO_2 NS and α-Fe_2O_3/CeO_2NS.

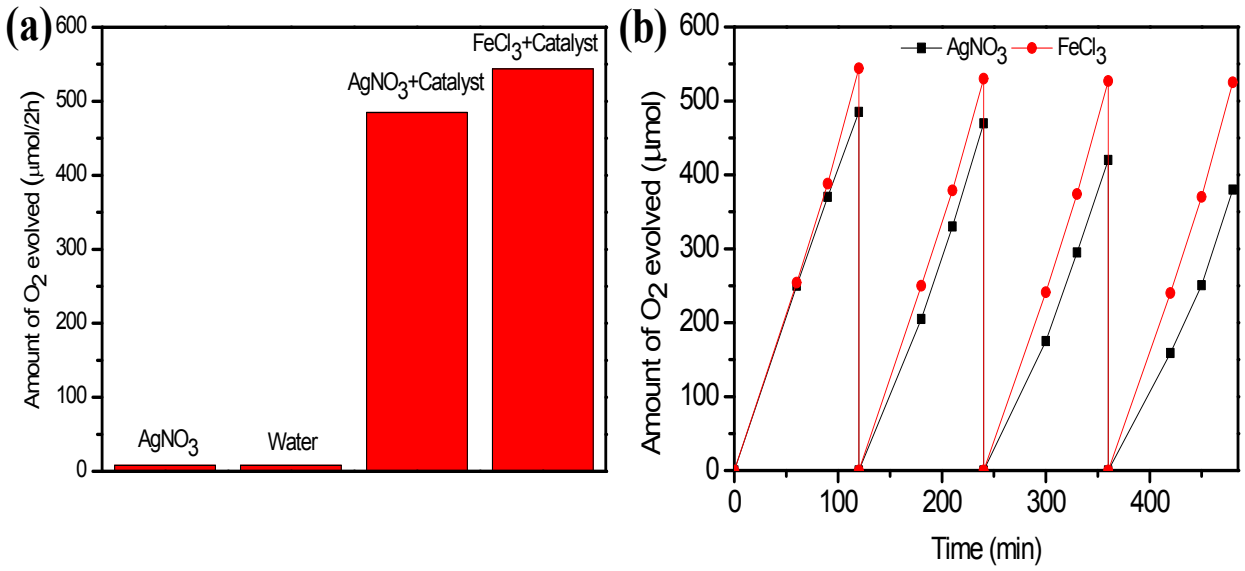

Fig. S6 (a) O_2 evolution experiment carry on two sacrificial reagent $AgNO_3$ and $FeCl_3$ solution, (b) Reusibility plot of FeOOH-CeO_2

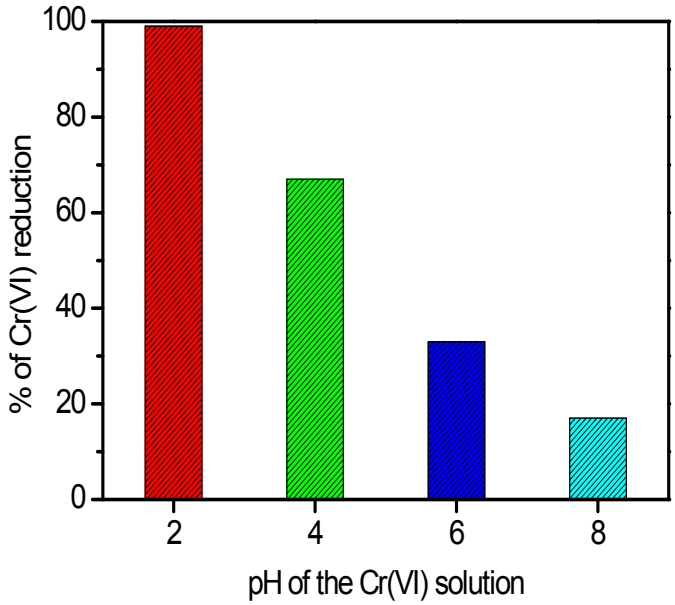

Fig. S7 (a) Effect of pH on the photo-reduction of Cr(VI) by α-FeOOH/CeO_2NS

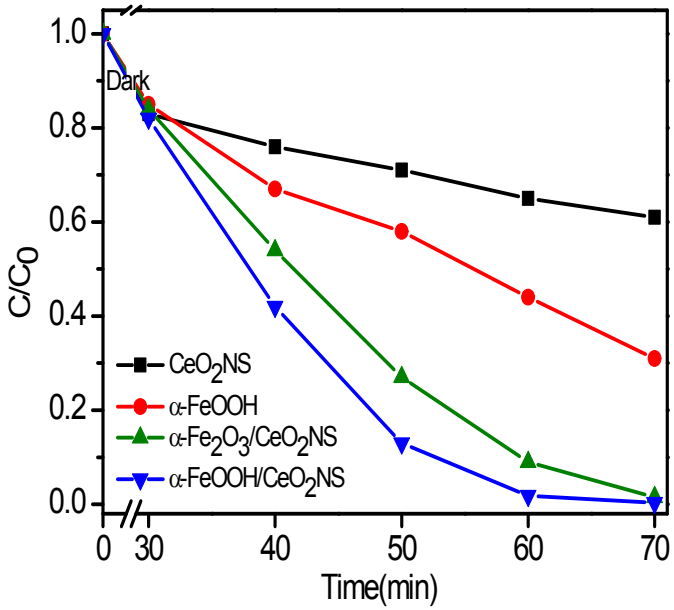

Fig. S7 (b) Photoreduction of Cr(VI) by CeO_2NS, α-FeOOH, α-FeOOH/CeO_2NS and α-Fe_2O_3/CeO_2NS.

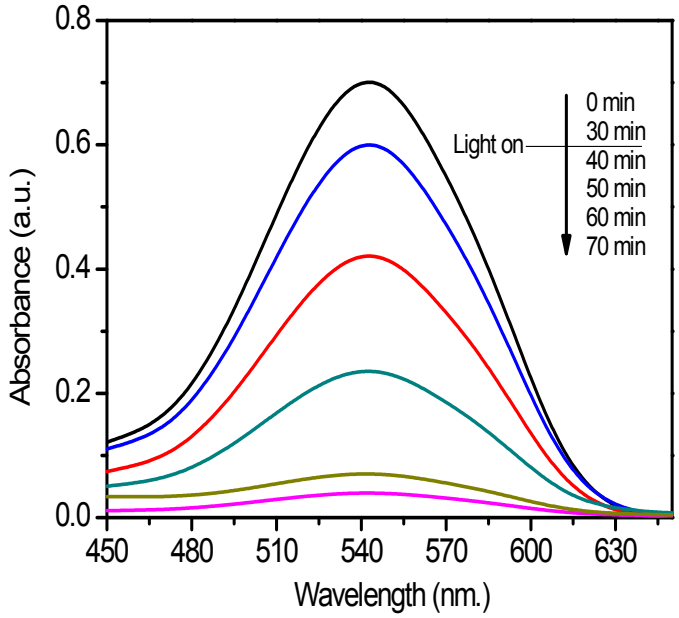

Fig. S7 (c) Concentration change of Cr(VI)-DPC as a function of time in presence of α-FeOOH/CeO_2NS.

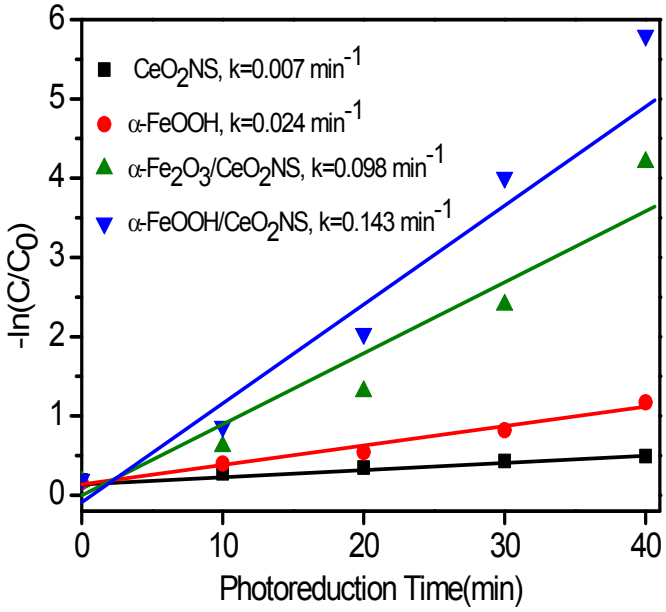

Fig. S7 (d) Kinetic study of photocatalytic Cr(VI) reduction over α-FeOOH/CeO_2NS.

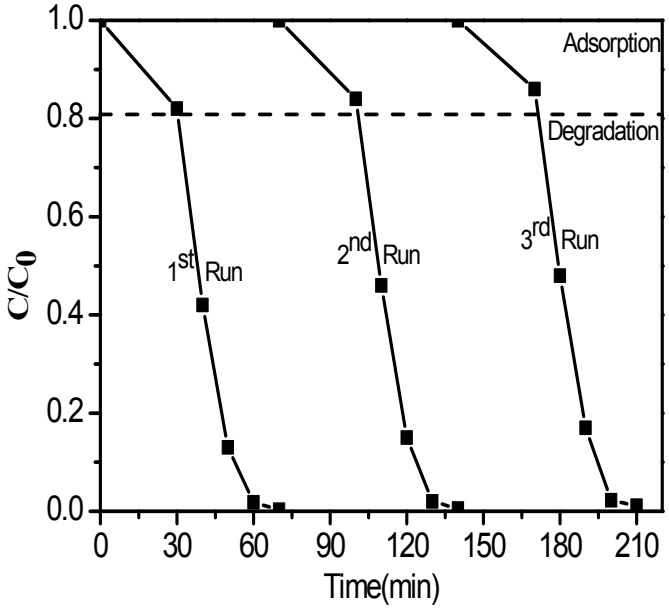

Fig. S7 (e) Reusability study of photocatalytic Cr(VI) reduction over α-FeOOH/CeO_2NS.

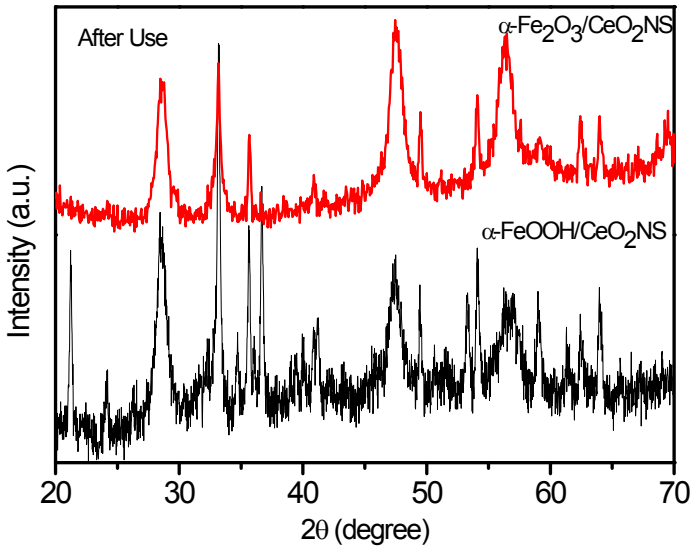

Fig. S8 XRD plot of α-FeOOH/CeO_2NS and α-Fe_2O_3/CeO_2NS after photocatalytic reaction.

References

1. (a). Y. Li, Z. Liu, Y. Wu, J. Chen, J. Zhao, F. Jin and P. Na, *Appl. Catal. B: Environ.,* 2018, **224,** 508-517. (b). Q. Meng, Y. Zhou, G. Chen, Y. Hu, C. Lv, L. Qiang and W. Xing, *Chem. Eng. J.,* 2018, **334,** 334-343.